Cardiovascular Research Advance Access published February 4, 2014

Cardiovascular Research
doi:10.1093/cvr/cvu011

Defective autophagosome trafficking contributes to impaired autophagic flux in coronary arterial myocytes lacking CD38 gene

Yang Zhang[1†], Ming Xu[1†], Min Xia[1], Xiang Li[1], Krishna M. Boini[1], Mi Wang[1], Erich Gulbins[2], Paul H. Ratz[3], and Pin-Lan Li[1*]

[1]Department of Pharmacology and Toxicology, Medical College of Virginia Campus, Virginia Commonwealth University, VA 23298, USA; [2]Department of Molecular Biology, Medical School Essen, University of Duisburg-Essen, Essen 45122, Germany; and [3]Department of Biochemistry and Molecular Biology and Pediatrics, Medical College of Virginia Campus, Virginia Commonwealth University, VA 23298, USA

Received 29 September 2013; revised 13 January 2014; accepted 14 January 2014

Time for primary review: 37 days

Aim Autophagic flux is an important process during autophagy maturation in smooth muscle cells. However, the molecular mechanisms underlying autophagic flux in these cells are largely unknown. Here, we revealed a previously undefined role of CD38, an enzyme that metabolizes $NADP^+$ into NAADP, in the regulation of autophagic flux in coronary arterial myocytes (CAMs).

Methods and results *In vivo* CD38 gene knockout mice ($CD38^{-/-}$) fed the high-fat Western diet showed increased accumulation of autophagosomes in coronary arterial media compared with that in wild-type ($CD38^{+/+}$) mice, suggesting that CD38 gene deletion results in a defective autophagic process in CAMs of coronary arteries. In primary cultured CAMs, CD38 gene deletion markedly enhanced 7-ketocholesterol (7-Ket, an atherogenic stimulus and autophagy inducer)-induced accumulation of autophagosomes and increased expression of an autophagic marker, LC3B. However, no difference in autophagosome formation was observed between $CD38^{+/+}$ and $CD38^{-/-}$ CAMs when autophagic flux was blocked, which indicates that CD38 regulates autophagic flux rather than induction of autophagosome formation. Further, 7-Ket-induced formation of autophagolysosomes was markedly attenuated in $CD38^{-/-}$ CAMs compared with $CD38^{+/+}$ CAMs. Mechanistically, CD38 gene deletion markedly inhibited 7-Ket-induced dynein activation and autophagosome trafficking, which were associated with attenuated lysosomal Ca^{2+} release. Importantly, coronary arterial smooth muscle from $CD38^{-/-}$ mice fed the Western diet exhibited phenotypic changes towards a more dedifferentiated state with abnormal extracellular matrix metabolism.

Conclusion Taken together, these results suggest that CD38 plays a critical role in autophagosome trafficking and fusion with lysosomes, thus controlling autophagic flux in CAMs under atherogenic stimulation.

Keywords Autophagic flux • CD antigens • Lysosomal signalling • Vascular smooth muscle

1. Introduction

Autophagy (or macroautophagy) is a tightly controlled cellular catabolic mechanism that eukaryotes use to degrade long-lived proteins and organelles.[1] The molecular mechanisms or regulatory pathways for autophagy have been extensively studied since the discovery of mammalian autophagy genes (Atg genes), and significant advances have been made to reveal its roles under physiological and pathological conditions.[2] It has been demonstrated that autophagy processes include induction and formation of autophagosome and autophagic flux, the latter of which consists of autophagosomes trafficking and fusion with lysosomes to form autophagolysosomes and breakdown of autophagic contents in autophagolysosomes.[3,4] Recent studies have indicated that augmented autophagy in the vascular smooth muscle cells (SMCs) plays an important role in atherosclerosis, which may be both protective and detrimental during atherosclerosis, depending on the status of autophagy or the

† Y.Z. and M.X. contributed equally to this work.

* Corresponding author. Tel: +1 8048284793; fax: +1 8048284794, Email: pli@vcu.edu

stage of atherosclerosis.[5] Increased but controlled autophagy in vascular SMCs at the early developmental stage of atherosclerosis may be beneficial via inducing a more differentiated and contractile phenotype, thereby decreasing cell proliferation and preventing fibrosis.[6] On the other hand, excessive autophagy in vascular SMCs of the fibrous cap that surrounds the necrotic core of atherosclerotic plaques may cause autophagic or type II cell death increasing the instability of atherosclerotic plaques,[7,8] which ultimately evokes atherothrombosis, myocardial infarction, or stroke.[9,10] Although the role of augmented autophagy in atherosclerosis has been extensively studied, there is no evidence that a defective or reduced autophagy is involved in the pathogenesis of atherosclerosis. Specifically, the molecular mechanisms for deregulated autophagic flux as well as their pathophysiological relevance are poorly understood.

CD38 is a multifunctional enzyme responsible for the production and metabolism of cyclic ADP-ribose (cADPR) and NAADP in vascular cells, which play important roles in the regulation of vascular function.[11] cADPR, an alternative Ca^{2+}-mobilizing second messenger to inositol 1,4,5-trisphosphate [Ins(1,4,5)P3], plays a crucial role in the regulation of multiple cell functions under physiological conditions.[12,13] Activation of the CD38/cADPR pathway contributes to the M_1 receptor agonist-induced Ca^{2+} release from the sarcoplasmic reticulum (SR) in coronary arterial myocytes (CAMs) and vasoconstriction in coronary arteries.[14] NAADP is another key product of CD38-ADP-ribosylcyclase and is reported to be the most potent intracellular Ca^{2+}-mobilizing signalling molecule.[15] In arterial SMCs, NAADP mobilizes intracellular Ca^{2+} in a two-pool mechanism that NAADP releases Ca^{2+} from a lysosome-dependent Ca^{2+} store, which serves as a localized signal to trigger Ca^{2+}-induced Ca^{2+} release leading to global Ca^{2+} increases in the cytosol.[16] Such NAADP-sensitive lysosome-derived Ca^{2+} and consequent increases in cytosolic Ca^{2+} have been shown to participate in the physiological regulation of cell functions or activities in a variety of tissues or cells.[15,17,18] In particular, autophagosomes trafficking and fusion with lysosomes has been shown to be a Ca^{2+}-dependent event.[19–21] Thus, we wonder whether the CD38-mediated Ca^{2+} signalling could control the formation of autophagolysosomes during autophagic flux in CAMs through regulation of autophagosomes trafficking and fusion with lysosomes.

In the present study, we used both *in vitro* and *in vivo* approaches to test this hypothesis. Our data first demonstrate that genetic deficiency of CD38 results in a defective autophagic process in coronary arterial media of mice fed the high-fat Western diet. Then, in primary cultured CAMs, we reveal that such defective autophagy under atherogenic stimulation is due to impaired autophagic flux, which is associated with attenuated lysosomal Ca^{2+} release, reduced dynein activation, and deregulated autophagososomes trafficking and fusion with lysosomes. Lastly, we demonstrate that coronary arterial smooth muscle from $CD38^{-/-}$ mice fed the Western diet exhibited phenotypic changes towards a more dedifferentiated state with abnormal extracellular matrix metabolism.

2. Materials

2.1 Animal procedure

Both $CD38^{-/-}$ and wild-type ($CD38^{+/+}$) mice on C57BL/6 background were purchased from the Jackson Laboratory. $CD38^{+/+}$ and $CD38^{-/-}$ mice (8 weeks of age; male) were fed 10-week normal diet or Western diet containing (g%): protein 20, carbohydrate 50, and fat 21 (Dytes, Bethlehem, PA, USA), as described previously.[22] Mice were sacrificed by cervical dislocation under ether anaesthesia. The hearts with coronary artery were obtained for coronary dissection or frozen in liquid nitrogen for preparation of frozen section slides. All experimental protocols were reviewed and approved by the Animal Care Committee of Virginia Commonwealth University. All animals were provided standard rodent chow and water ad libitum in a temperature-controlled room.

2.2 Western blot analysis

Western blot analysis was performed as described previously[23] and also in Supplementary material online. Primary antibodies used are rabbit anti-LC3B (dilution 1:1000, Cell Signaling Technology), rabbit anti-Beclin1 (dilution 1:1000, Abcam), rabbit anti-calponin (1:500, Santa Cruz), mouse anti-vimentin (1:500, Santa Cruz), goat anti-β-actin (1:500, Santa Cruz), or anti-β-tubulin (1:1000, Santa Cruz).

2.3 Primary cell culture of mouse CAMs and treatments

CAMs were isolated from $CD38^{+/+}$ or $CD38^{-/-}$ mice as previously described[24] and also discussed in Supplementary material online. The expression of CD38 in $CD38^{+/+}$ or $CD38^{-/-}$ CAMs was examined by western blot (see Supplementary material online, *Figure S1*). Cells were treated with 7-ketocholesterol (7-Ket) (Sigma; 10 μg/mL) or rapamycin (RPM) (Sigma; 20 nM) for 24 h, or left starved in Earle's balanced salt solution (Invitrogen) for 2 h at 37°C. The dosages of 7-Ket and RPM were chosen based on our pilot study that cell death was barely observed at these dosages but induces submaximal autophagy in CAMs.

2.4 Electron microscopy

The sample preparations for electron microscopy including fixation and staining were performed according to the published method.[25] Autophagic vacuoles and lysosomes were examined by a Jeol JEM-1230 transmission electron microscope (TEM) equipped with a Gatan UltraScan 4000SP 4K × 4 K CCD camera.

2.5 Flow cytometric detection of autophagosomes and autophagolysosomes

Autophagosome formation in cells was detected using a CytoID Autophagy Detection Kit (Enzo, Plymouth Meeting, PA, USA) following manufacturer's instructions. The CytoID fluorescent reagents specifically detect the autophagic vacuoles formed during autophagy. Briefly, cells were trypsinized, spun down, and washed twice in phenol red-free RPMI 1640 with 2% foetal bovine serum (FBS). The cells were resuspended in 0.5 mL of freshly diluted CytoID reagents and incubated at 37°C for 30 min. The CytoID fluorescence of cells was immediately analysed by flow cytometry using a flow cytometer (GUAVA, Hayward, CA, USA). The percentage of cells with CytoID staining was used to represent the relative formation or accumulation of autophagosomes.

The autophagolysosome formation was analysed by flow cytometry using a lysosomotrophic dye and acridine orange.[26] Acridine orange accumulates in acidic vesicles such as lysosomes to display red fluorescence, but is green fluorescent in neutral environments such as in the cytosol and nuclei. Since autophagolysosomes are larger acidic compartments compared with lysosomes, increased fusion of lysosomes with autophagosomes to form autophagolysosomes will increase the red-to-green fluorescence intensity ratio. Briefly, cells were stained with acridine orange (2 μg/mL) for 17 min and washed twice in

phenol red-free RPMI 1640 with 2% FBS. Then the ratio of red-to-green fluorescence intensity from cells was obtained by flow cytometry to indicate the change of intracellular autophagolysosomes. In some groups, CAMs were transfected with Atg7siRNA or the control scrambled siRNA, as described previously.[27]

2.6 Fluorescence resonance energy transfer analysis

Cells were stained with fluorescein isothiocyanate (FITC)-labelled antibody against Lamp1 (1 : 200, BD Biosciences) and MitoTracker probes (Invitrogen), which label mitochondrial proteins. An acceptor bleaching protocol was used to measure the fluorescence resonance energy transfer (FRET) efficiency between FITC/MitoTracker, as described previously[28,29] and also in Supplementary material online.

2.7 Assay for autophagic flux using tandem RFP-GFP-LC3B

The autophagic flux in CAMs was assayed using the Premo^{TM} Autophagy Tandem Sensor red fluorescent protein (RFP)-green fluorescent protein (GFP)-LC3B kit (Invitrogen) following manufacturer's instructions. Briefly, 10^4 cells grown in coverslips were incubated with 6 μL BacMam reagents containing tandem RFP-GFP-LC3B DNA overnight (>16 h) and then treated as indicated. The cells were washed and bathed in phosphate buffered saline (PBS) and visualized through sequentially scanning on an Olympus laser scanning confocal microscope (Fluoview FV1000, Olympus, Japan). The number of LC3B-positive autophagosomes and autophagolysosomes in merged images was quantitated using ImageJ.

2.8 Assays for lysosomal pH, protease activity, and cathepsins

To observe lysosomal alkalinization, we incubated CAMs in PBS buffer with or without 100 μM chloroquine for 30 min. The cells were then loaded with LysoSensor Green DND-189 (1 μM; Invitrogen) in PBS buffer for 15 min at 37°C. Cells were washed twice with PBS and immediately visualized with a confocal laser scanning microscope (Fluoview FV1000, Olympus, Japan).

The enzyme activity of lysosomal proteases in CAMs was assayed for their ability to process DQ-BSA Red (a derivative of BSA, the red fluorescence of which is quenched unless it is cleaved by proteolytic enzymes), as described previously.[30] Briefly, CAMs were incubated with DQ-BSA Red (10 μg/mL) for 2 h at 37°C and the mean fluorescence intensity of these cells was determined by flow cytometry. The catalytic activities of cathepsin B (Abcam, Inc.) and cathepsin D (Sigma) were determined using commercially available kits following manufacturer's instructions.

2.9 Assay of cytoplasmic dynein ATPase activity and dynamic analysis of autophagosome movement in CAMs

Dynein in mouse CAMs was purified and its ATPase activity was assayed, as described previously[31] and also in Supplementary material online. To monitor the autophagosome movement, CAMs were incubated with BacMam GFP-LC3B virus particles (Invitrogen) at 37°C for overnight (>16 h) to express the LC3B-GFP gene. The confocal fluorescent microscopic recording was conducted with an Olympus Fluoview System, as described previously[32] and also in Supplementary material online. The number of cells with different velocity of autophagosomes was calculated.

2.10 Fluorescence measurement of intracellular [Ca^{2+}] in CAMs

A fluorescence image analysis system was used to determine intracellular [Ca^{2+}] in CAMs with fura-2 acetoxymethyl ester (fura-2) as an indicator, as described previously[33] and also discussed in Supplementary material online. Lysosomal Ca^{2+} release was monitored indirectly by treating fura-2-loaded CAMs with glycyl-L-phenylalanine 2-naphthylamide (GPN; 200 μM), a tripeptide causing osmotic lysis of cathepsin C-positive lysosomes. Ultrasound (Rich-Mar Sonitron 2000) and Optison (Perflutren protein type A microspheres) were employed to deliver NAADP into CAMs for determination of its effect on $[Ca^{2+}]_i$, as described previously[33] and also discussed in Supplementary material online.

2.11 Statistics

Data are presented as means ± SEM. Significant differences in mean values between- and within-multiple groups were examined using analysis of variance (ANOVA), any significant difference revealed by this procedure were further investigated using Tukey's multiple-range test. Student's *t*-test was used to detect significant difference between two groups. The statistical analysis was performed by the SigmaStat 3.5 software (Systat Software, Chicago, IL, USA). $P < 0.05$ was considered statistically significant.

3. Results

3.1 Effects of CD38 gene deletion on autophagy in coronary arterial media of mice

To test the significance of CD38 in autophagy *in vivo*, we examined the expression of an autophagy marker, LC3B, in coronary arterial media from $CD38^{+/+}$ and $CD38^{-/-}$ mice fed the Western diet. As shown in *Figure 1A*, LC3B was highly increased in the coronary arterial wall of $CD38^{-/-}$ mice compared with $CD38^{+/+}$ mice particularly with the Western diet. In the homogenates of dissected coronary arteries isolated from mice fed with the Western diet, the expression of LC3B and another autophagy marker Beclin1 were much higher in $CD38^{-/-}$ mice than those in $CD38^{+/+}$ mice (*Figure 1B*). LC3B is recruited to autophagosomal membranes during the formation of autophagosomes. Once autophagosomes fuse with lysosomes to form autophagolysosomes, LC3B in the autophagolysosomal lumen is degraded by the lysosomal proteases. Therefore, increases in the expression of LC3B suggest more autophagosomes are formed and/or less LC3B proteins are degraded due to impaired autophagic flux. Nonetheless, these results implicate that CD38 gene deletion results in the defective autophagic process in coronary arterial media of mice.

3.2 $CD38^{-/-}$ CAMs exhibit impaired autophagy upon atherogenic stimulation

We next determined whether CD38 gene deletion results in autophagy deregulation in primary cultured CAMs. CAMs were treated with 7-Ket, since it is a prototype atherogenic stimulus abundant in oxidized low-density lipoprotein and enhances the expression of LC3B and autophagy in vascular smooth muscle cells.[34] RPM is used as a positive control, which induces autophagosome formation by inhibiting the activity of mTOR complex 1 (mTORC1),[35,36] and promotes autophagosome fusion with lysosome and subsequent autophagic flux.[37,38] The formation of autophagosomes and autophagolysosomes was directly

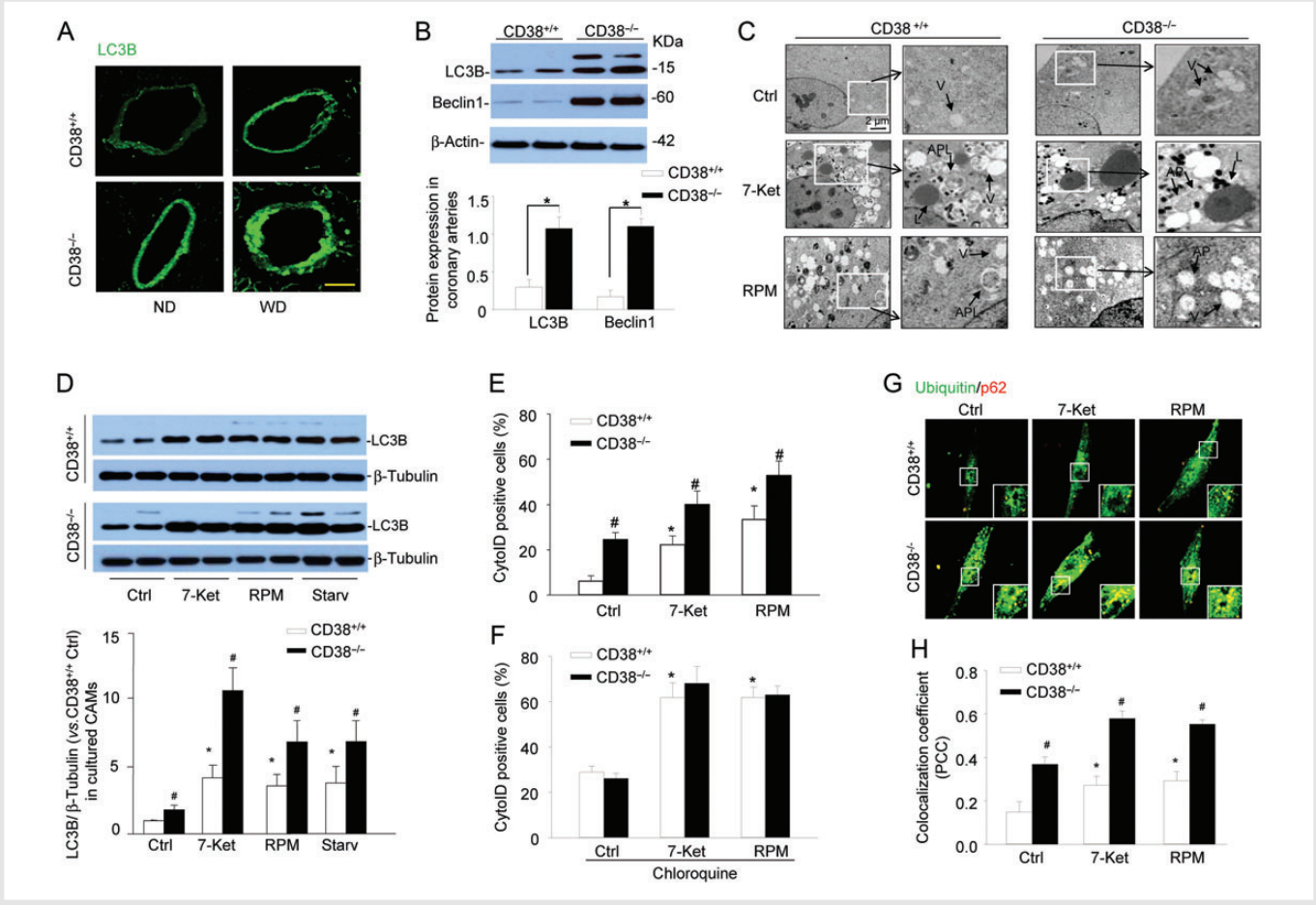

Figure 1 Deregulated autophagic process in coronary arterial smooth muscle of $CD38^{-/-}$ and in $CD38^{-/-}$ CAMs upon atherogenic stimulation. (*A*) $CD38^{+/+}$ and $CD38^{-/-}$ mice were fed normal diet or a high-fat Western diet for 10 weeks. Representative confocal fluorescence images for LC3B are shown ($n = 4$ mice). Scale bar: 50 μm. (*B*) Representative western blot gel documents and summarized data showing the protein expression of LC3B, Beclin1 and β-actin in the homogenates of coronary arteries from $CD38^{+/+}$ and $CD38^{-/-}$ mice fed WD. Data are shown means ± SEM of values from six mice ($^{*}P < 0.05$). (*C*) Representative electron microscope images showing the formation of autophagosomes and autophagolysosomes in $CD38^{+/+}$ and $CD38^{-/-}$ CAMs under control condition (Ctrl) or treated with atherogenic stimulus 7-Ket(10 μg/mL) or RPM(20 nM) for 24 h ($n = 3$). (*D*) Representative western blot gel documents and summarized data showing the protein expression of LC3B and β-tubulin in $CD38^{+/+}$ and $CD38^{-/-}$ CAMs under control condition (Ctrl) or treated with 7-Ket, RPM, or under starvation. (*E* and *F*) Mouse CAMs were stained with CytoID fluorescent probes that detect intracellular autophagosomes. Summarized per cent of CytoID stained cells showing the relative number of autophagosomes in $CD38^{+/+}$ and $CD38^{-/-}$ CAMs without (*E*) or with (*F*) an autophagic flux inhibitor, chloroquine. (*G* and *H*) Representative confocal images and summarized colocalization coefficient showing the colocalization of ubiquitin with p62. Summarized data in (*D*)–(*F*), and (*H*) are shown means ± SEM of values from six independent experiments. $^{*}P < 0.05$ vs. control of $CD38^{+/+}$ CAMs and $^{\#}P < 0.05$ vs. $CD38^{+/+}$ CAMs with the same treatment by two-way ANOVA with Tukey's *post hoc* test.

observed under TEM (*Figure 1C*). Both $CD38^{+/+}$ and $CD38^{-/-}$ CAMs exhibited many vacuoles with or without myelin and mitochondria debris when stimulated by 7-Ket or RPM, suggesting increased formation of autophagosomes. In $CD38^{+/+}$ CAMs, there were many autophagolysosomes detected upon stimulation of 7-Ket and RPM, which were characterized by lysosomes merging with vacuoles, suggesting the occurrence of lysosome fusion to autophagosomes. However, in $CD38^{-/-}$ CAMs, no autophagolysosomes could be seen although many autophagosomes (vacuoles) also seen in electron microscopy (EM) studies. It appears that $CD38^{-/-}$ CAMs exhibit impaired autophagy with reduced formation of autophagolysosomes upon atherogenic stimulation. Since these EM studies were not quantitative, we confirmed the impaired autophagolysosome formation in $CD38^{-/-}$ CAMs by another series of biochemical and fluorescent assays. First, western blot analysis shows that in $CD38^{-/-}$ CAMs, the abundance of LC3B was more marked in $CD38^{-/-}$ CAMs than $CD38^{+/+}$ CAMs when they were challenged by the atherogenic agent 7-Ket or classical autophagy stimulators such as RPM or starvation (*Figure 1D*).

To analyse the dynamic balance between autophagosomes formation and autophagic flux, CAMs were stained with CytoID probes that detect autophagic vacuoles including pre-autophagosomes, autophagosomes, or autophagolysosomes. Enhanced induction of autophagosome formation or impaired autophagic flux will result in an increased number of autophagic vacuoles and enhances CytoID fluorescence. As shown in *Figure 1E*, in $CD38^{+/+}$ CAMs 7-Ket or RPM stimulation significantly increased the percentage of CytoID-positive cells, which was

further augmented in $CD38^{-/-}$ CAMs. Similarly, inhibition of CD38 activity by nicotinamide markedly enhanced 7-Ket-induced increase in CytoID-positive cells (see Supplementary material online, *Figure S2*). However, in the presence of chloroquine, a lysosome inhibitor that blocks autophagic flux, no difference in 7-Ket- or RPM-induced increase in CytoID-positive cells was observed between $CD38^{+/+}$ and $CD38^{-/-}$ CAMs (*Figure 1F*). Thus, these results suggest that CD38 gene deletion impairs autophagic flux but not induction of autophagosome formation in CAMs under atherogenic stimulation leading to accumulation of autophagosomes.

Inclusion of granular ubiquitin or a selective autophagy substrate p62 in autophagosomes of cells can be used to detect the breakdown of autophagic vesicles.[26] Increase in ubiquitin and p62 in autophagosomes suggests a failed breakdown of autophagosomes. As shown in *Figure 1G* and *H*, compared with $CD38^{+/+}$ CAMs, $CD38^{-/-}$ CAMs exhibited much more yellow puncta (insert of each image), suggesting that more ubiquitin and p62 proteins were accumulated in autophagosomes, in particular, when cells were stimulated by 7-Ket or RPM. These results further indicate that reduced autophagolysosome formation in $CD38^{-/-}$ CAMs, resulting in an impaired breakdown process of autophagic vesicles and accumulation of autophagosomes.

3.3 Decreased formation of autophagolysosomes in $CD38^{-/-}$ CAMs

Next, the formation of autophagolysosomes was analysed by flow cytometry studies on cells that were labelled with acridine orange, which accumulates in lysosomes with red fluorescence and shows green fluorescence in the cytoplasm and the nucleus.[26] *Figure 2A* shows that $CD38^{+/+}$ CAMs treated with 7-Ket or RPM shifted up to the area with high-red fluorescence intensity, which was inhibited in $CD38^{-/-}$ CAMs. The quantification of the data shows that 7-Ket or RPM significantly increased the red-to-green fluorescence ratio, indicating the formation of autophagolysosomes (*Figure 2B*). Further, gene silencing of Atg7, an essential protein for autophagy induction,[39] completely abolished 7-Ket or RPM-induced increases in the red-to-green fluorescence ratio, suggesting that these ratio increases by 7-Ket or RPM are indeed due to increased formation of autophagolysosomes (*Figure 2C*). However, $CD38^{-/-}$ cells failed to respond with the formation of autophagolysosomes upon treatment with 7-Ket or RPM, indicating that CD38 function is required for the formation of autophagolysosomes (*Figure 2B*). Lastly, increased lysosome biogenesis in CAMs may also enhance lysosomal accumulation of acridine orange and increase the red-to-green fluorescence ratio. However, no difference in protein expression in Lamp1, a lysosome marker, was found between $CD38^{+/+}$ and $CD38^{-/-}$ CAMs under control condition or with 7-Ket or RPM stimulation (data not shown), which suggests that CD38 is not involved in lysosome biogenesis.

By confocal microscopic co-localization and FRET detection, we directly observe the fusion of autophagosomes with lysosomes in $CD38^{+/+}$ and $CD38^{-/-}$ CAMs. *Figure 2D* depicts that 7-Ket or RPM markedly increased the FRET (blue fluorescence) between Lamp1 (FITC labelled) and mitochondrial proteins aggregated in autophagosomes (MitoTracker labelled) in $CD38^{+/+}$ CAMs, indicating increased fusion of lysosomes with autophagosomes. However, such increases in FRET were much lower in $CD38^{-/-}$ CAMs compared with those in $CD38^{+/+}$ CAMs. The summarized FRET efficiency further confirms that the presence of the CD38 gene is essential for the control of lysosome fusion with autophagosomes in CAMs (*Figure 2E*).

To directly monitor the autophagic flux in living CAMs, we introduced a tandem RFP-GFP-LC3B gene into cells to express LC3B protein fused with both RFP and GFP in tandem. The tandem RFP-GFP-LC3B protein contains an acid-sensitive GFP (green fluorescence is quenched in acidic environments) and an acid-insensitive RFP (red fluorescence remains in acidic environments). Thus, the maturation from an autophagosome (neutral pH) to the autophagolysosome (with an acidic pH) can be visualized by imaging specific loss of the GFP fluorescence upon acidification of the autophagosome following lysosomal fusion. In this respect, yellow/orange puncta in the merged image (colocalization of both GFP and RFP) represent autophagosomes and red puncta in the merged image (RFP only since acidification abolishes GFP fluorescence) correspond to autophagolysosomes. As shown in *Figure 2F*, 7-Ket markedly increased the number of yellow/orange puncta (autophagosomes) and red puncta (autophagolysosomes) in the merged image in $CD38^{+/+}$ CAMs. However, in $CD38^{-/-}$ CAMs, 7-Ket significantly increased the number of yellow/orange puncta (autophagosomes), but very few red puncta (autophagolysosomes) could be observed. The quantified data in *Figure 2G* and *H* indicate that impaired autophagic flux by CD38 deficiency was due to defective maturation of autophagosomes to autophagolysosomes.

3.4 Effects of CD38 gene deletion on lysosomal pH and protease activity of CAMs

We next examined whether CD38 deficiency affects autophagic flux via alteration in lysosome acidification and its protease activity. Lysosomal pH was determined by staining CAMs with LysoSensor Green DND-189, which accumulates in acidic organelles and exhibits green fluorescence. $CD38^{-/-}$ CAMs exhibit a similar green fluorescence to $CD38^{+/+}$ CAMs, indicating that CD38 deficiency does not impair lysosomal acidification (*Figure 3A*). Chloroquine is known to alkalize the lysosome, which decreased LysoSensor fluorescence intensity in $CD38^{+/+}$ and $CD38^{-/-}$ CAMs (*Figure 3A*). The lysosomal protease activity was assayed for their ability to process DQ-BSA Red. The red fluorescence of DQ-BSA Red is quenched unless it is cleaved by proteolytic enzymes. As shown in *Figure 3B*, 7-Ket did not alter DQ-BSA Red fluorescence in CAMs and no difference in DQ-BSA Red fluorescence was found between $CD38^{+/+}$ and $CD38^{-/-}$ CAMs treated with control or 7-Ket, while lysosomal activity was marked inhibited by chloroquine (*Figure 3B*). Consistently, CD38 deficiency did not affect activities of cathepsin B and D in CAMs (*Figure 3C* and *D*).

3.5 Inhibited dynein ATPase and autophagosome movement in $CD38^{-/-}$ CAMs upon 7-Ket stimulation

Dynein is a motor protein responsible for nearly all minus-end microtubule-based transport of vesicles in eukaryotic cells and has recently been implicated in autophagosomes trafficking to meet with the lysosomes to form autophagolysosomes. Thus, we examined whether CD38 deficiency results in deregulated dynein activation and autophagosomes trafficking during atherogenic stimulation. Indeed, treatment of CAMs with 7-Ket resulted in a markedly increase in dynein ATPase activity in $CD38^{+/+}$ CAMs, which was significantly attenuated in $CD38^{-/-}$ CAMs (*Figure 4A*). Autophagosomes are formed randomly throughout the cytoplasm and then transported to lysosomes, the majority of which is localized in the perinuclear region. To monitor the autophagosome movement to lysosomes, we labelled autophagosomes with LC3B-GFP by the BacMam technique and determined the velocity of

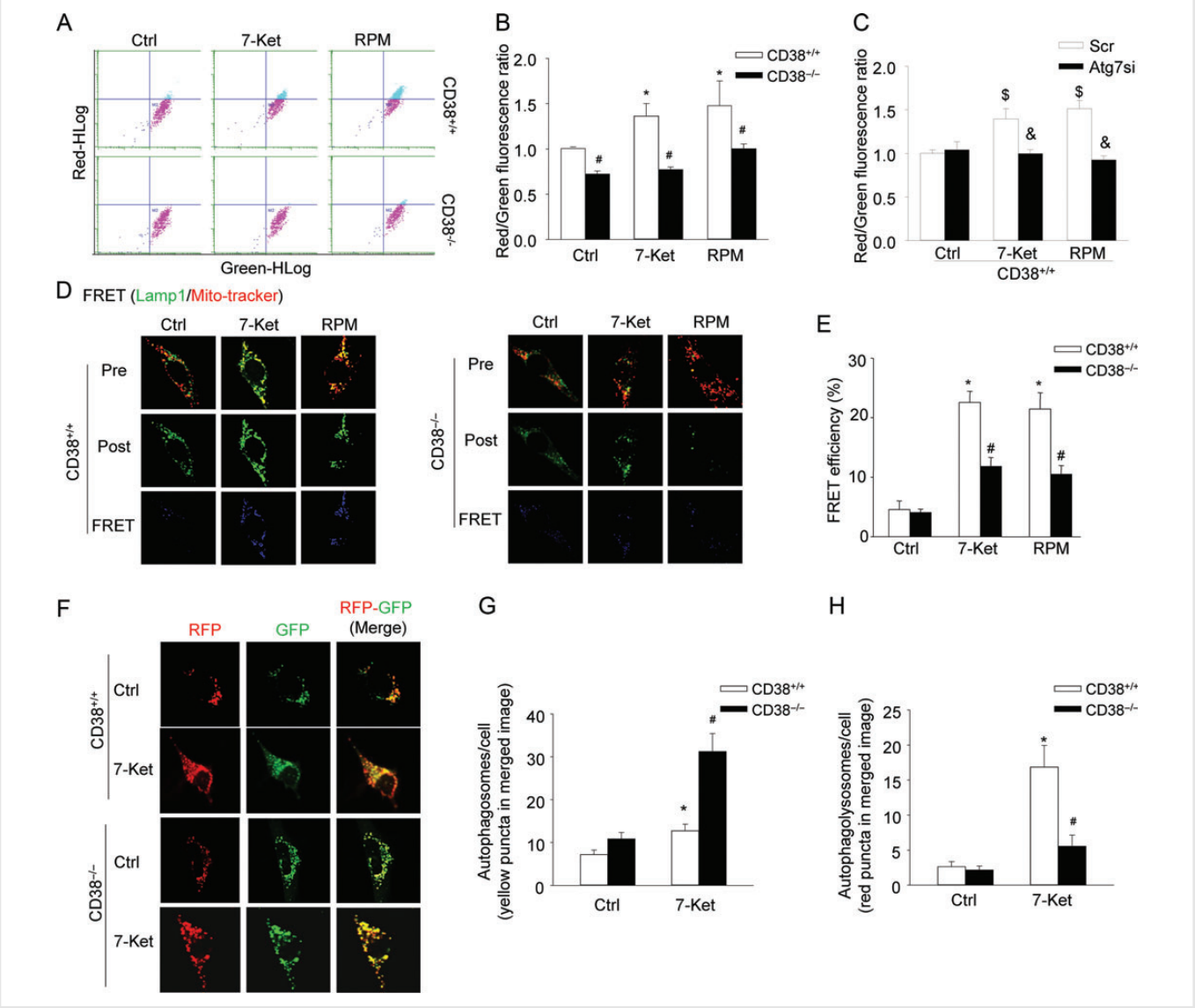

Figure 2 Decreased formation of autophagolysosomes, lack of lysosome fusion with autophagosomes and inhibited autophagic flux in CD38$^{-/-}$ CAMs under atherogenic stimulation. (*A* and *B*) Mouse CAMs were treated as indicated and stained with acridine orange (2 μg/mL) for 17 min. Representative dot plots of flow cytometry analysis (*A*) and summarized red-to-green fluorescence ratio of acridine orange staining (*B*) showing the formation of autophagolysosomes in CD38$^{+/+}$ and CD38$^{-/-}$ CAMs ($n = 6$). (*C*) The summarized red-to-green fluorescence ratio shows the acridine orange staining in CD38$^{+/+}$ CAMs transfected with scramble or Atg7 siRNA (Atg7si) ($n = 6$). (*D* and *E*) Representative confocal images of FRET (*D*) and summarized FRET efficiency (*E*) between FITC-Lamp1 and MitoTracker. The FRET images were obtained by the subtraction of pre-bleaching (Pre) images from the post-bleaching (Post) images and shown in a dark blue colour. Increased intensity of blue colour represents a higher level of FRET in these cells ($n = 6$). (*F*–*H*) Representative confocal images of the tandem RFP-GFP-LC3B transfected CAMs show the formation of autophagosomes and autophagolysosomes. Autophagosomes were visualized as yellow or orange puncta (RFP-GFP-LC3B) in merged images (far right images in *F*), whereas red puncta (RFP-LC3B) in merged images represent autophagolysosomes since acidification abolishes green fluorescence. (*G* and *H*) Summarized data showing the number of autophagosomes (yellow/orange puncta) and autophagolysosomes (red puncta) in the merged images ($n = 4$). Data are shown means ± SEM of values from four or six independent experiments as indicated in each panel. $^{*}P < 0.05$ vs. control of CD38$^{+/+}$ CAMs; $^{\#}P < 0.05$ vs. CD38$^{+/+}$ CAMs with the same treatment; $^{\$}P < 0.05$ vs. control of scramble transfected CD38$^{+/+}$ CAMs; $^{\&}P < 0.05$ vs. scramble with the same treatment by two-way ANOVA with Tukey's *post hoc* test.

autophagosome movement. Under control condition, autophagosomes moved bi-directionally, i.e. towards and away from the nucleus, and no difference was found in velocity of autophagosome movement between CD38$^{+/+}$ and CD38$^{-/-}$ CAMs (*Figure 4B*). In CD38$^{+/+}$ CAMs, 7-Ket significantly enhanced the autophagosome movement in the velocity range between 0.01 and 0.09 mm/s (*Figure 4C*). In contrast, such 7-Ket-enhanced autophagosome movement was blocked in CD38$^{-/-}$ CAMs (*Figure 4C*).

3.6 Attenuated lysosomal Ca^{2+} release response in CD38$^{-/-}$ CAMs upon 7-Ket stimulation

We further tested whether inhibited dynein activation and AP trafficking in CD38$^{-/-}$ CAMs were associated with deregulated lysosomal Ca^{2+} signalling. To this end, fluorescent imaging analysis was conducted to monitor lysosomal Ca^{2+} release indirectly by treating fura-2-loaded

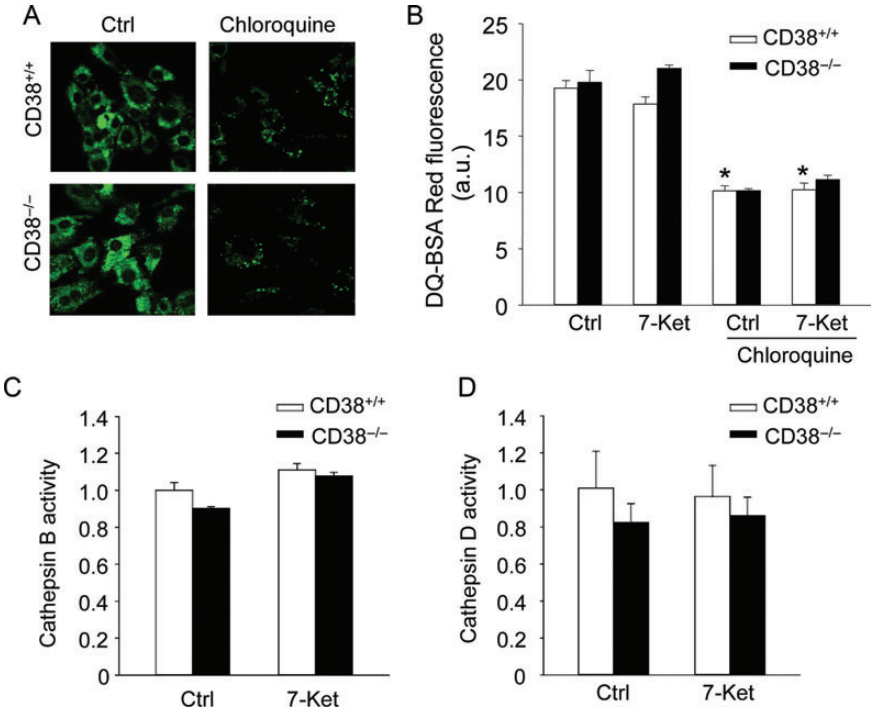

Figure 3 Effects of CD38 deficiency on lysosomal pH and protease activity in CAMs. (*A*) $CD38^{+/+}$ and $CD38^{-/-}$ CAMs were treated with chloroquine (100 μM) for 30 min or left untreated. They were then stained with LysoSensor Green DND-189 and analysed by a fluorescence microscopy. Representative fluorescence images from four independent experiments are shown. (*B*) $CD38^{+/+}$ and $CD38^{-/-}$ CAMs were stained with DQ-BSA Red probes, the red fluorescence of which is quenched and can be dequenched when it is cleaved by lysosomal protease. Summarized data for DQ-BSA Red fluorescence intensity show the lysosomal protease activity in $CD38^{+/+}$ and $CD38^{-/-}$ CAMs with or without chloroquine (100 μM). (*C* and *D*) Summarized data show the catalytic activities for lysosomal cathepsin (*B*) and (*D*) in $CD38^{+/+}$ or $CD38^{-/-}$ CAMs. Data are shown means ± SEM of values from four independent experiments. $^{*}P < 0.05$ vs. control of $CD38^{+/+}$ CAMs. $^{\#}P < 0.05$ vs. $CD38^{+/+}$ CAMs with the same treatment by two-way ANOVA with Tukey's *post hoc* test.

CAMs with 200 μM GPN. GPN was used to release Ca^{2+} from lysosomes by inducing their selective osmotic swelling. As shown in *Figure 5A* and *B*, GPN-induced Ca^{2+} release was significantly enhanced in $CD38^{+/+}$ CAMs with 7-Ket treatment, which was markedly blocked in $CD38^{-/-}$ CAMs or by the specific lysosome function blocker bafilomycin (Baf). In addition, we determined whether such enhanced lysosomal Ca^{2+} release potential was associated with elevated basal cytosolic Ca^{2+} concentration in CAMs (without GPN treatment). As shown in *Figure 5C*, 7-Ket significantly increased the basal cytosolic [Ca^{2+}], which was attenuated by Baf. CD38 deficiency had no effect on the basal cytosolic [Ca^{2+}] under resting condition; however, 7-Ket-induced increases in basal cytosolic [Ca^{2+}] were markedly inhibited in $CD38^{-/-}$ cells. Direct delivery of CD38 product, NAADP, induced similar Ca^{2+} release in $CD38^{-/-}$ and $CD38^{+/+}$ CAMs, suggesting that Ca^{2+} release machinery in lysosomes remains intact in $CD38^{-/-}$ CAMs (*Figure 5D*). We recently reported that NAADP regulate lysosomal Ca^{2+} release in CAMs through the transient receptor potential (TRP)-ML1 (mucolipin-1) channels.[33,40] Similar to CD38 deficiency, silencing of the TRPML1 gene by transfecting TRPML1 shRNA plasmids (Origene) significantly enhanced 7-Ket-induced accumulation of autophagosomes (*Figure 5E*) and decreased 7-Ket-induced autophagolysosomes formation (*Figure 5F*) in CAMs from $CD38^{+/+}$ mice.

3.7 CD38 deficiency decreases contractile phenotype and increase collagen deposition in coronary arteries

As shown in *Figure 6A*, representative fluorescent images qualitatively demonstrated that the expression of a contractile phenotype marker calponin (green staining) in coronary arteries decreased in $CD38^{-/-}$ mice compared with that in $CD38^{+/+}$ mice, particularly when they were on the Western diet. $CD38^{-/-}$ mice exhibited little yellow staining suggesting that less calponin expressed in the area of higher LC3B expression. In contrast, as shown in *Figure 6B*, $CD38^{-/-}$ mice had increased the abundance of vimentin, a dedifferentiation-associated filament protein, in coronary arterial media, where LC3B was high, as shown by a deep yellow staining. Western blot analysis (*Figure 6C*) confirmed that in dissected coronary arteries from mice with the Western diet, the expression of calponin was lower, whereas vimentin was higher in $CD38^{-/-}$ mice compared with $CD38^{+/+}$ mice. These results demonstrate that coronary arterial smooth muscle in $CD38^{-/-}$ mice had an enhanced dedifferentiated phenotype to that in $CD38^{+/+}$ mice. The extracellular matrix was visualized by TEM using a trichrome collagen stain kit (Sigma) and the blue colour intensity of each image was analysed by the Image Pro Plus 6.0 software (Media Cybernetics, Rockville, MD, USA). As shown in *Figure 6D*, the coronary arterial wall in $CD38^{-/-}$

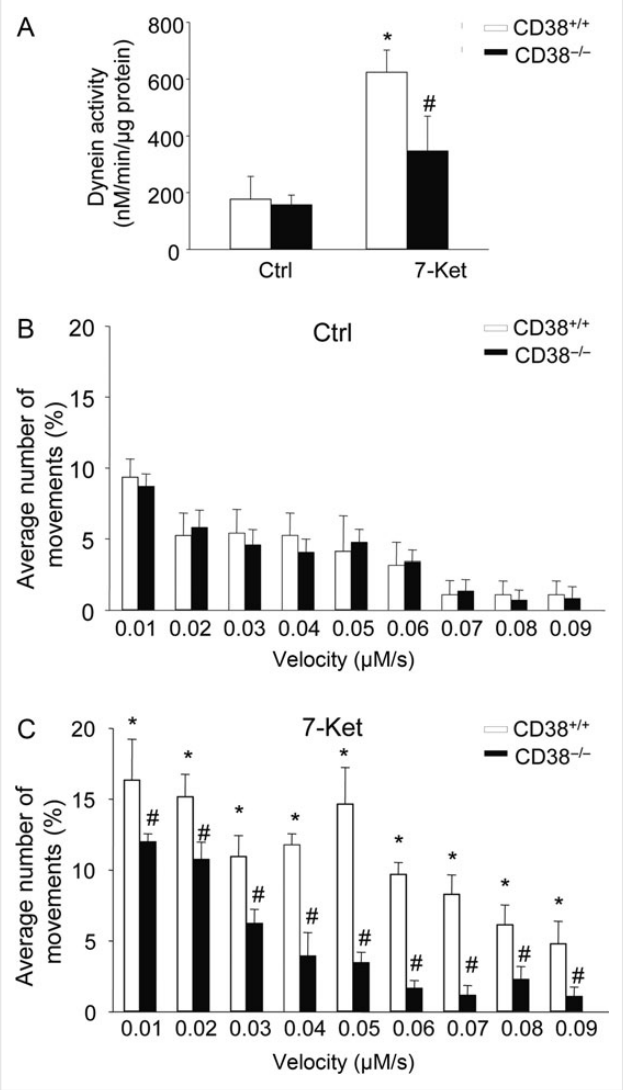

Figure 4 Dynein activity and autophagosome dynamic movements in CAMs. (*A*) Summarized data showing the dynein ATPase activity in $CD38^{+/+}$ and $CD38^{-/-}$ CAMs under control condition or with 7-Ket stimulation. Data are shown means ± SEM of values from four independent experiments. $^{*}P < 0.05$ vs. control of $CD38^{+/+}$ CAMs. $^{\#}P < 0.05$ vs. $CD38^{+/+}$ CAMs with the same treatment by two-way ANOVA with Tukey's *post hoc* test. (*B* and *C*) The summarized data show the velocity of autophagosomes in $CD38^{+/+}$ and $CD38^{-/-}$ CAMs under control (*B*) or treated with 7-Ket (*C*). Data are shown means ± SEM of values from four independent experiments. $^{*}P < 0.05$ vs. control of $CD38^{+/+}$ CAMs with the same velocity; $^{\#}P < 0.05$ vs. $CD38^{+/+}$ CAMs with the same treatment and velocity by two-way ANOVA with Tukey's *post hoc* test.

mice showed increased collagen expression, particularly when mice were fed the Western diet, indicating increases in the extracellular matrix.

4. Discussion

The present study demonstrated that in CAMs, CD38 gene deletion results in an impaired autophagic flux characterized by accumulation of autophagosomes and reduced formation of autophagolysosomes. Such impaired autophagic flux was associated with blunted NAADP/lysosomal Ca^{2+}, dynein activation, and autophagosomes trafficking in CAMs.

The hallmark of autophagy is the formation of the autophagosomes, followed by its fusion with a lysosome, termed autophagolysosomes. Microtubule-associated protein 1 light chain (LC3) exists in the cytoplasm in a soluble form (LC3A). A phosphatidylethanolamine-conjugated form of LC3 (LC3B) is associated with the phagophore and the inner autophagosomal membrane and is a highly specific marker for these structures.[41] Upon fusion with the lysosome, LC3B on the inner autophagosomal membrane is degraded.[3] The present study attempted to explore the mechanisms that regulate autophagic flux in the pathogenesis of atherosclerosis. Here, we demonstrated that CD38 gene deletion increased LC3B protein levels in coronary arterial media in mice fed the Western diet and in primary cultured CAMs under atherogenic stimulation by 7-Ket. These *in vivo* and *in vitro* results implicate that under atherogenic stimulation, loss of CD38 function causes deregulated autophagic process in CAMs with more autophagosomes formed or accumulated. Indeed, the accumulation of autophagosomes, reduced lysosome fusion with autophagosomes, and decreased autophagolysosomes formation were directly observed in $CD38^{-/-}$ CAMs by EM.

Our data further confirmed that accumulation of autophagosomes is due to impaired autophagic flux but not increased formation. First, we used a Cyto-ID Green detection reagent, which is a novel dye that selectively labels autophagic vacuoles in live cells and quantitatively monitors autophagic flux.[27] This novel method confirms the finding in the EM study that 7-Ket stimulation accumulates more autophagosomes in $CD38^{-/-}$ CAMs than $CD38^{+/+}$ cells. Importantly, the difference in autophagosome accumulation was not observed in the presence of an autophagic flux blocker, choloquine, suggesting that CD38 is not involved in autophagy induction and formation of autophagosomes. Inclusion of granular ubiquitin or p62 in autophagosomes of cells is a valuable non-EM-based technique to detect increased autophagy, in particular, for detection of the breakdown of autophagic vesicles. Our data revealed that $CD38^{-/-}$ CAMs had more ubiquitin and p62 in autophagosomes than those in $CD38^{+/+}$ cells suggests a failed breakdown of autophagosomes in $CD38^{-/-}$ CAMs. Thus, these results support the view that autophagic flux rather than induction of autophagosome formation is deregulated in CAMs lacking CD38 gene.

Based on our data from acridine orange staining, FRET between Lamp1 and Mitotracker, and a tandem RFP-GFP-LC3B assay, we found that genetic deficiency of CD38 can decrease the fusion of autophagosomes with lysosomes leading to reduced formation of autophagolysosomes. Acridine orange staining indirectly shows a decrease in autophagolysosome formation in $CD38^{-/-}$ CAMs (*Figure 2A–C*). Autophagosome fusion with lysosomes was also observed by FRET detection (blue fluorescence) between Lamp1 (FITC labelled) and mitochondrial proteins aggregated in autophagosomes (MitoTracker labelled) (*Figure 2D* and *E*). Our data suggest that the lack of the CD38 gene blunted the fusion of autophagosomes with lysosomes in CAMs. Moreover, using a tandem RFP-GFP-LC3B assay, we further demonstrated that the maturation of autophagosomes to autophagolysosomes was blocked in the absence of CD38 (*Figure 2F*). In another aspect, the decrease in autophagic flux can be due to defective lysosomal proteolytic activity that inhibits autophagosome turnover.[30] However, our data from Lysosensor staining (*Figure 3A*), DQ-BSA Red assay (*Figure 3B*), and *in vitro* cathepsin substrate assay (*Figure 3C* and *D*) confirmed that lysosomal pH, lysosomal protease activity, and cathepsins B and D

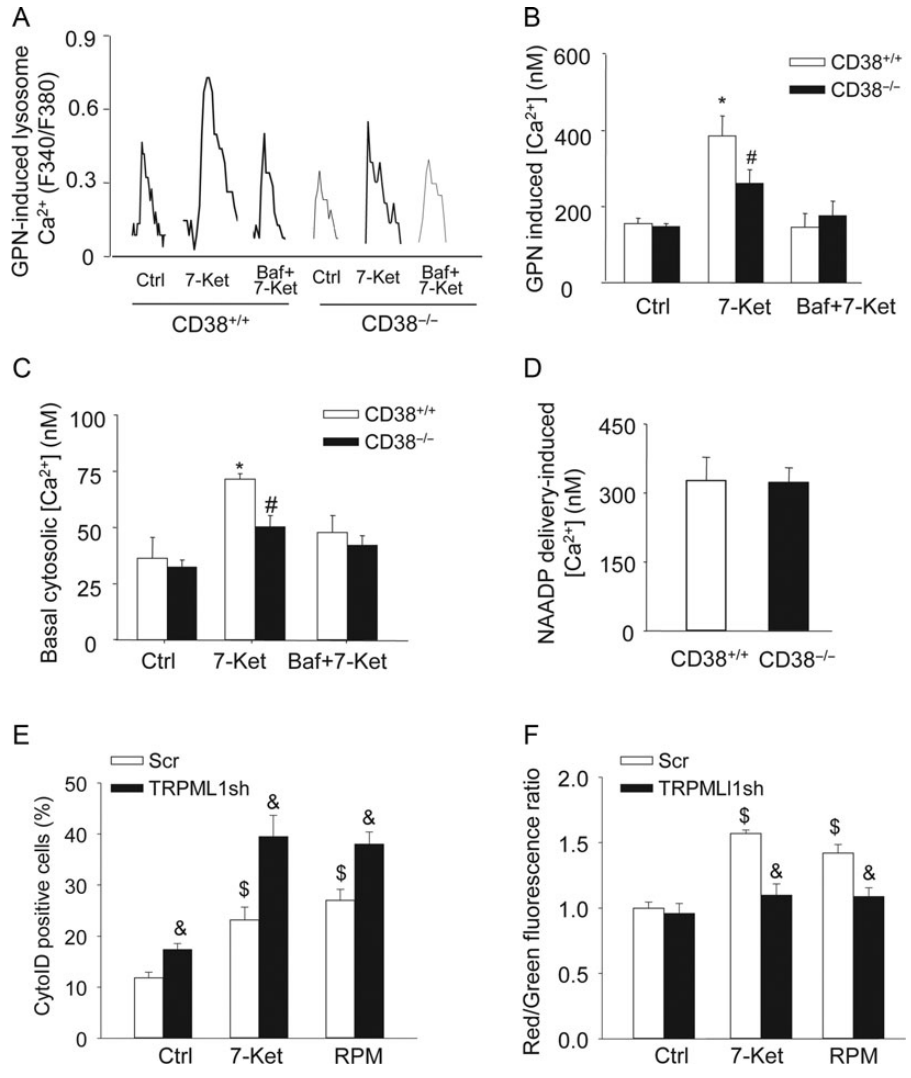

Figure 5 Lysosome Ca^{2+} release in response to atherogenic stimuli in living CAMs. GPN (200 μM) was used to release Ca^{2+} from lysosomes. Representative lysosomal Ca^{2+} traces (*A*) and quantification of lysosomal Ca^{2+} release responses (*B*) show the effects of the CD38 deficiency or lysosome inhibitor Baf (10 nM) on GPN-induced lysosomal Ca^{2+} release in CAMs ($n = 5$). (*C*) The basal cytosolic Ca^{2+} concentrations ($[Ca^{2+}]$) in CAMs treated with 7-Ket in the presence of the absence of bafilomycin (without GPN) ($n = 5$). (*D*) Effects of direct delivery of NAADP on intracellular Ca^{2+} response in $CD38^{+/+}$ and $CD38^{-/-}$ CAMs ($n = 3$). (*E*) Summarized per cent of Cyto-ID stained cells showing the relative number of autophagosomes in $CD38^{+/+}$ CAMs with scramble (Scr) or TRPML1 shRNA (TRPML1sh) transfection ($n = 4$). (*F*) The summarized red-to-green fluorescence ratio of acridine orange staining showing the formation of autophagolysosomes in $CD38^{+/+}$ CAMs with scramble or TRPML1 shRNA transfection ($n = 4$). Data are shown means ± SEM of values from three to five independent experiments as indicated in each panel. $^{*}P < 0.05$ vs. control of $CD38^{+/+}$ CAMs; $^{\#}P < 0.05$ vs. $CD38^{+/+}$ CAMs with the same treatment; $^{\$}P < 0.05$ vs. control of scramble transfected $CD38^{+/+}$ CAMs; $^{\&}P < 0.05$ vs. scramble with the same treatment by two-way ANOVA with Tukey's *post hoc* test.

activity remain unchanged in $CD38^{-/-}$ CAMs under control or 7-Ket stimulation compared with those in $CD38^{+/+}$ CAMs. Thus, these data excluded the involvement of lysosomal acidification or lysosomal protease activity in the impaired autophagic flux in $CD38^{-/-}$ CAMs.

During autophagy, autophagosomes move vectorially towards the centrosome, where lysosomes are usually concentrated.[38] Recent studies have demonstrated that autophagosomes can move in a microtubule- and dynein-dynactin motor complex-dependent manner.[42] Here, we demonstrated that CD38 deficiency inhibited 7-Ket induced dynein activation in CAMs. We further found that the movement of autophagosomes within a cell was enhanced in 7-Ket-treated $CD38^{+/+}$ CAMs, which was prevented in $CD38^{-/-}$ CAMs. These results implicate that CD38 function is needed for dynein to control lysosome–autophagosome fusion and the formation of autophagolysosomes. Previous studies have reported that direct binding of Ca^{2+} to a component of the dynein complex regulates dynein motor function and the distribution of cytoplasmic dynein.[43,44] Lysosomes contain high levels of Ca^{2+}, which serves as an important intracellular Ca^{2+} store similar to the SR.[45] Lysosomal Ca^{2+} can be mobilized or released to mediate molecular trafficking or recycling and to control vesicular fusion events associated with lysosomes.[46,47] NAADP, a CD38-ADP-ribosylcyclase product, is one of the most potent intracellular Ca^{2+}-mobilizing molecules, which mobilizes intracellular Ca^{2+} release in a two-pool mechanism depending upon a

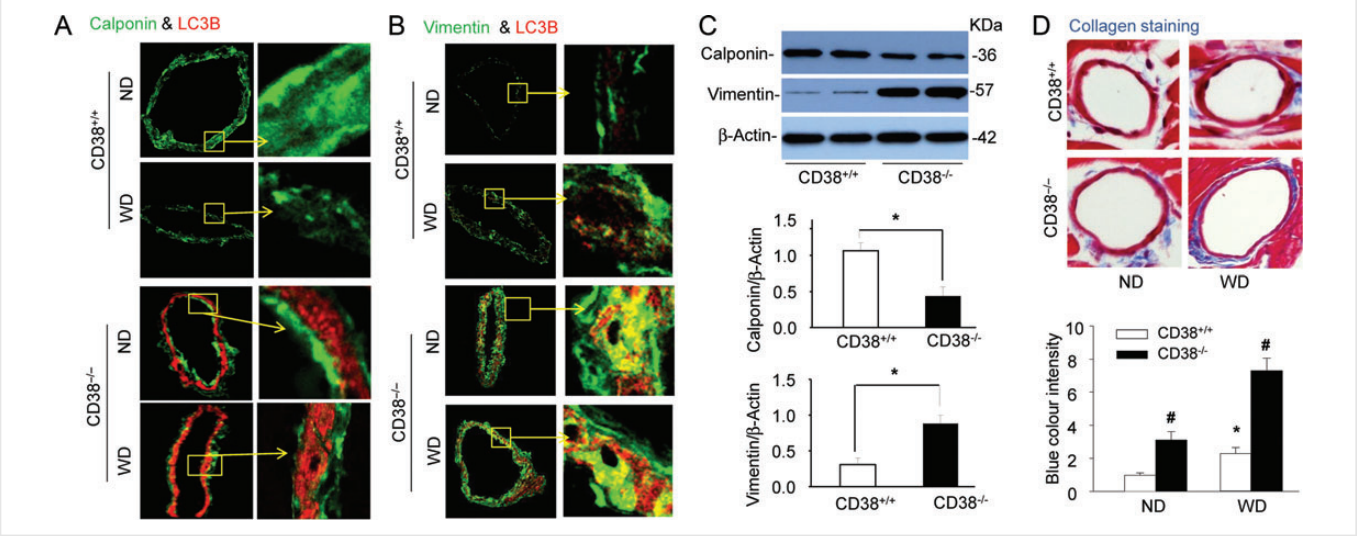

Figure 6 CD38 deficiency decreases contractile phenotype and increase collagen deposition in coronary arteries. CD38$^{+/+}$ and CD38$^{-/-}$ mice were fed normal diet (ND) or a high-fat Western diet (WD) for 10 weeks. Coronary arteries of mouse hearts were dissected and used for western blot analysis and confocal immunofluorescent analysis. (*A* and *B*) Representative confocal fluorescence images for co-staining of calponin with LC3B (*A*) or vimentin with LC3B (*B*) in coronary arteries of mice fed ND or WD ($n = 4$ mice). (*C*) Representative western blot gel documents and summarized data showing the protein expression of calponin, vimentin, and β-actin in the homogenates of dissected coronary arteries from CD38$^{+/+}$ and CD38$^{-/-}$ mice fed WD. Data are shown means ± SEM of values from six mice ($^{*}P < 0.05$). (*D*) Trichrome staining of the coronary arterial wall showing the collagen staining (blue colour) and summarized blue colour intensity the coronary arterial wall of mice. Data are shown means ± SEM of values from six mice. $^{*}P < 0.05$ vs. CD38$^{+/+}$ mice with normal diet; $^{\#}P < 0.05$ vs. CD38$^{+/+}$ mice with the same diet by two-way ANOVA with Tukey's *post hoc* test.

lysosome-dependent Ca^{2+} store in arterial SMCs.[15,16] Mechanistically, NAADP may regulate lysosomal Ca^{2+} release and lysosome function through its action on the TRP-ML1 (mucolipin-1) channels, as we reported recently, or through other mechanisms such as two-pore channels.[33,40] NAADP has been recognized as a fundamental signalling mechanism, regulating a variety of cell or organ functions in different biological systems.[15] For example, in coronary arteries, we recently demonstrated that FasL activated CD38 and increased NAADP production, but FasL itself did not produce vasoconstriction.[48] However, FasL significantly enhanced IP3-producing agonist U46619-induced coronary arterial contraction, suggesting that activation of CD38/NAADP signalling may sensitize arterial contraction.[48] In the present study, we demonstrated that atherogenic stimulation by 7-Ket enhanced lysosomal Ca^{2+} release in CD38$^{+/+}$ CAMs, which was markedly attenuated in CD38$^{-/-}$ CAMs. Such enhanced lysosomal Ca^{2+} release potential was associated with elevated basal cytosolic Ca^{2+} concentration in CD38$^{+/+}$ CAMs, which is consistent with a previous study showing that 7-Ket triggers a sustained increase in cytosolic Ca^{2+} in cultured human vascular SMCs.[49] Deficiency of TRPML1 results in impaired lysosome trafficking and autophagolysosomal degradation in human fibroblasts.[50] Here, we also demonstrated that silencing of lysosomal Ca^{2+} channel TRPML1 mimics the effects of CD38 deficiency on autophagosome accumulation and autophagolysosomes formation in CAMs. Further, we confirmed that lysosomal Ca^{2+} release machinery is intact in CD38$^{-/-}$ CAMs. Thus, these results indicate that impaired autophagic flux in CD38$^{-/-}$ CAMs is a consequence of insufficient CD38-mediated NAADP production. Together, our data, for the first time, link lysosome deregulation due to the absence of CD38-NAADP-Ca^{2+} signalling to impaired dynein function and subsequent defective autophagic flux in CAMs.

The role of vascular SMCs in cardiovascular diseases including atherosclerosis relates to their proliferative and secretory property, whereby they proliferate, grow, and migrate into intima and produce extracellular matrix to induce fibrosis. Defective autophagic flux may influence cell signalling pathways such as Wnt activity leading to fibrosis[51] or collagen degradation in cardiomyoctes.[51] Here, we demonstrated an increased expression of a dedifferentiation marker, vimentin, decreased expression of a contractile phenotype marker, calponin, and increased collagen deposition in the coronary arteries of CD38$^{-/-}$ mice, particularly when these mice were fed WD. Our study may provide a novel notion how defective autophagic flux due to impaired CD38 function may contribute to the development of atherogenesis. Atherogenic stimuli such as 7-Ket activate autophagy to form autophagosomes in arterial SMCs, where dynein-mediated trafficking (probably along with microtubules[52]) and fusion between autophagosomes and lysosomes, are controlled by CD38/NAADP-mediated regulation in lysosomal TRPML1-Ca^{2+} leading to effective autophagic flux. This CD38-regulated autophagic flux protects SMCs from atherosclerotic injury upon atherogenic stimulations possibly via down-regulation of signalling pathways controlling cell dedifferentiation, proliferation, and growth, or levels of extracellular matrix proteins via autophagolysosomal degradation machinery. When the controlling mechanism of lysosome function is insufficient due to impaired CD38 function, the autophagic flux is impaired, which may activate cell dedifferentiation, proliferation, and growth, thereby stimulating production of extracellular matrix and ultimately contribute to coronary arterial smooth muscle remodelling accelerating atherosclerosis.

In summary, the role of CD38 in autophagic flux is associated with CD38-regulated lysosomal Ca^{2+} and dynein activation. Defect in the CD38-NAADP-Ca^{2+} signalling pathway results in impaired autophagic flux, which promotes CAM dedifferentiation and stimulates the production of the extracellular matrix, which ultimately may result in coronary arterial smooth muscle remodelling contributing to atherosclerosis.

Our data provide new insights into how CD38-NAADP-Ca^{2+} signalling and its regulated lysosome function contribute to autophagy and phenotype switching in CAMs leading to vascular smooth muscle remodelling.

Supplementary material

Supplementary material is available at *Cardiovascular Research* online.

Conflict of interest: none declared.

Funding

This study was supported by grants from the National Institute of Health (HL057244, HL075316, and HL091464).

References

1. Ryter SW, Lee SJ, Smith A, Choi AM. Autophagy in vascular disease. *Proc Am Thorac Soc* 2010;**7**:40–47.
2. Bampton ET, Goemans CG, Niranjan D, Mizushima N, Tolkovsky AM. The dynamics of autophagy visualized in live cells: from autophagosome formation to fusion with endo/lysosomes. *Autophagy* 2005;**1**:23–36.
3. Xie Z, Klionsky DJ. Autophagosome formation: core machinery and adaptations. *Nat Cell Biol* 2007;**9**:1102–1109.
4. Reggiori F, Klionsky DJ. Autophagy in the eukaryotic cell. *Eukaryot Cell* 2002;**1**:11–21.
5. Libby P. Atherosclerosis: disease biology affecting the coronary vasculature. *Am J Cardiol* 2006;**98**:3Q–9Q.
6. Lacolley P, Regnault V, Nicoletti A, Li Z, Michel JB. The vascular smooth muscle cell in arterial pathology: a cell that can take on multiple roles. *Cardiovasc Res* 2012;**95**:194–204.
7. Jia G, Cheng G, Agrawal DK. Differential effects of insulin-like growth factor-1 and atheroma-associated cytokines on cell proliferation and apoptosis in plaque smooth muscle cells of symptomatic and asymptomatic patients with carotid stenosis. *Immunol Cell Biol* 2006;**84**:422–429.
8. Martinet W, De Bie M, Schrijvers DM, De Meyer GR, Herman AG, Kockx MM. 7-ketocholesterol induces protein ubiquitination, myelin figure formation, and light chain 3 processing in vascular smooth muscle cells. *Arterioscler Thromb Vasc Biol* 2004;**24**:2296–2301.
9. Virmani R, Kolodgie FD, Burke AP, Farb A, Schwartz SM. Lessons from sudden coronary death: a comprehensive morphological classification scheme for atherosclerotic lesions. *Arterioscler Thromb Vasc Biol* 2000;**20**:1262–1275.
10. Clarke M, Bennett M. The emerging role of vascular smooth muscle cell apoptosis in atherosclerosis and plaque stability. *Am J Nephrol* 2006;**26**:531–535.
11. Teggatz EG, Zhang G, Zhang AY, Yi F, Li N, Zou AP *et al*. Role of cyclic ADP-ribose in Ca^{2+}-induced Ca^{2+} release and vasoconstriction in small renal arteries. *Microvasc Res* 2005;**70**:65–75.
12. Guse AH, da Silva CP, Berg I, Skapenko AL, Weber K, Heyer P *et al*. Regulation of calcium signalling in T lymphocytes by the second messenger cyclic ADP-ribose. *Nature* 1999;**398**:70–73.
13. Young GS, Jacobson EL, Kirkland JB. Water maze performance in young male Long-Evans rats is inversely affected by dietary intakes of niacin and may be linked to levels of the NAD^+ metabolite cADPR. *J Nutr* 2007;**137**:1050–1057.
14. Ge ZD, Zhang DX, Chen YF, Yi FX, Zou AP, Campbell WB *et al*. Cyclic ADP-ribose contributes to contraction and Ca^{2+} release by M1 muscarinic receptor activation in coronary arterial smooth muscle. *J Vasc Res* 2003;**40**:28–36.
15. Galione A. NAADP, a new intracellular messenger that mobilizes Ca^{2+} from acidic stores. *Biochem Soc Trans* 2006;**34**:922–926.
16. Cancela JM, Churchill GC, Galione A. Coordination of agonist-induced Ca^{2+}-signalling patterns by NAADP in pancreatic acinar cells. *Nature* 1999;**398**:74–76.
17. Klionsky DJ, Cregg JM, Dunn WA Jr, Emr SD, Sakai Y, Sandoval IV *et al*. A unified nomenclature for yeast autophagy-related genes. *Dev Cell* 2003;**5**:539–545.
18. Brailoiu E, Hoard JL, Filipeanu CM, Brailoiu GC, Dun SL, Patel S *et al*. Nicotinic acid adenine dinucleotide phosphate potentiates neurite outgrowth. *J Biol Chem* 2005;**280**:5646–5650.
19. Ghavami S, Eshragi M, Ande SR, Chazin WJ, Klonisch T, Halayko AJ *et al*. S100A8/A9 induces autophagy and apoptosis via ROS-mediated cross-talk between mitochondria and lysosomes that involves BNIP3. *Cell Res* 2010;**20**:314–331.
20. Kim HJ, Soyombo AA, Tjon-Kon-Sang S, So I, Muallem S. The Ca(2+) channel TRPML3 regulates membrane trafficking and autophagy. *Traffic* 2009;**10**:1157–1167.
21. Li X, Gulbins E, Zhang Y. Oxidative stress triggers Ca-dependent lysosome trafficking and activation of acid sphingomyelinase. *Cell Physiol Biochem* 2012;**30**:815–826.
22. Bjursell M, Gerdin AK, Lelliott CJ, Egecioglu E, Elmgren A, Tornell J *et al*. Acutely reduced locomotor activity is a major contributor to Western diet-induced obesity in mice. *Am J Physiol Endocrinol Metab* 2008;**294**:E251–E260.
23. Zhang C, Boini KM, Xia M, Abais JM, Li X, Liu Q *et al*. Activation of Nod-like receptor protein 3 inflammasomes turns on podocyte injury and glomerular sclerosis in hyperhomocysteinemia. *Hypertension* 2012;**60**:154–162.
24. Xu M, Zhang Y, Xia M, Li XX, Ritter JK, Zhang F *et al*. NAD(P)H oxidase-dependent intracellular and extracellular O_2*- production in coronary arterial myocytes from CD38 knockout mice. *Free Radic Biol Med* 2012;**52**:357–365.
25. Swanson J, Bushnell A, Silverstein SC. Tubular lysosome morphology and distribution within macrophages depend on the integrity of cytoplasmic microtubules. *Proc Natl Acad Sci USA* 1987;**84**:1921–1925.
26. Raben N, Shea L, Hill V, Plotz P. Monitoring autophagy in lysosomal storage disorders. *Methods Enzymol* 2009;**453**:417–449.
27. Wei YM, Li X, Xu M, Abais JM, Chen Y, Riebling CR *et al*. Enhancement of autophagy by simvastatin through inhibition of Rac1-mTOR signaling pathway in coronary arterial myocytes. *Cell Physiol Biochem* 2013;**31**:925–937.
28. Li X, Han WQ, Boini KM, Xia M, Zhang Y, Li PL. TRAIL death receptor 4 signaling via lysosome fusion and membrane raft clustering in coronary arterial endothelial cells: evidence from ASM knockout mice. *J Mol Med (Berl)* 2013;**91**:25–36.
29. Jin S, Yi F, Zhang F, Poklis JL, Li PL. Lysosomal targeting and trafficking of acid sphingomyelinase to lipid raft platforms in coronary endothelial cells. *Arterioscler Thromb Vasc Biol* 2008;**28**:2056–2062.
30. Yue W, Hamai A, Tonelli G, Bauvy C, Nicolas V, Tharinger H *et al*. Inhibition of the autophagic flux by salinomycin in breast cancer stem-like/progenitor cells interferes with their maintenance. *Autophagy* 2013;**9**:714–729.
31. Paschal BM, Shpetner HS, Vallee RB. Purification of brain cytoplasmic dynein and characterization of its in vitro properties. *Methods Enzymol* 1991;**196**:181–191.
32. Xu M, Li XX, Xiong J, Xia M, Gulbins E, Zhang Y *et al*. Regulation of autophagic flux by dynein-mediated autophagosomes trafficking in mouse coronary arterial myocytes. *Biochim Biophys Acta* 2013;**1833**:3228–3236.
33. Zhang F, Zhang G, Zhang AY, Koeberl MJ, Wallander E, Li PL. Production of NAADP and its role in Ca^{2+} mobilization associated with lysosomes in coronary arterial myocytes. *Am J Physiol Heart Circ Physiol* 2006;**291**:H274–H282.
34. Ding Z, Wang X, Schnackenberg L, Khaidakov M, Liu S, Singla S *et al*. Regulation of autophagy and apoptosis in response to ox-LDL in vascular smooth muscle cells, and the modulatory effects of the microRNA hsa-let-7 g. *Int J Cardiol* 2013;**168**:1378–1385.
35. Neufeld TP. TOR-dependent control of autophagy: biting the hand that feeds. *Curr Opin Cell Biol* 2010;**22**:157–168.
36. Jung CH, Ro SH, Cao J, Otto NM, Kim DH. mTOR regulation of autophagy. *FEBS Lett* 2010;**584**:1287–1295.
37. Zhou C, Zhong W, Zhou J, Sheng F, Fang Z, Wei Y *et al*. Monitoring autophagic flux by an improved tandem fluorescent-tagged LC3 (mTagRFP-mWasabi-LC3) reveals that high-dose rapamycin impairs autophagic flux in cancer cells. *Autophagy* 2012;**8**:1215–1226.
38. Jahreiss L, Menzies FM, Rubinsztein DC. The itinerary of autophagosomes: from peripheral formation to kiss-and-run fusion with lysosomes. *Traffic* 2008;**9**:574–587.
39. Pattison JS, Osinska H, Robbins J. Atg7 induces basal autophagy and rescues autophagic deficiency in CryABR120G cardiomyocytes. *Circ Res* 2011;**109**:151–160.
40. Zhang F, Jin S, Yi F, Li PL. TRP-ML1 functions as a lysosomal NAADP-sensitive Ca^{2+} release channel in coronary arterial myocytes. *J Cell Mol Med* 2009;**13**:3174–3185.
41. Kabeya Y, Mizushima N, Ueno T, Yamamoto A, Kirisako T, Noda T *et al*. LC3, a mammalian homologue of yeast Apg8p, is localized in autophagosome membranes after processing. *EMBO J* 2000;**19**:5720–5728.
42. Kimura S, Noda T, Yoshimori T. Dynein-dependent movement of autophagosomes mediates efficient encounters with lysosomes. *Cell Struct Funct* 2008;**33**:109–122.
43. Lin SX, Collins CA. Regulation of the intracellular distribution of cytoplasmic dynein by serum factors and calcium. *J Cell Sci* 1993;**105**(Pt 2):579–588.
44. Lesich KA, Kelsch CB, Ponichter KL, Dionne BJ, Dang L, Lindemann CB. The calcium response of mouse sperm flagella: role of calcium ions in the regulation of dynein activity. *Biol Reprod* 2012;**86**:105.
45. Christensen KA, Myers JT, Swanson JA. pH-dependent regulation of lysosomal calcium in macrophages. *J Cell Sci* 2002;**115**:599–607.
46. Pryor PR, Mullock BM, Bright NA, Gray SR, Luzio JP. The role of intraorganellar Ca(2+) in late endosome-lysosome heterotypic fusion and in the reformation of lysosomes from hybrid organelles. *J Cell Biol* 2000;**149**:1053–1062.
47. Lloyd-Evans E, Waller-Evans H, Peterneva K, Platt FM. Endolysosomal calcium regulation and disease. *Biochem Soc Trans* 2010;**38**:1458–1464.
48. Zhang F, Xia M, Li PL. Lysosome-dependent Ca(2+) release response to Fas activation in coronary arterial myocytes through NAADP: evidence from CD38 gene knockouts. *Am J Physiol Cell Physiol* 2010;**298**:C1209–C1216.
49. Sasaki H, Watanabe F, Murano T, Miyashita Y, Shirai K. Vascular smooth muscle cell apoptosis induced by 7-ketocholesterol was mediated via Ca^{2+} and inhibited by the calcium channel blocker nifedipine. *Metabolism* 2007;**56**:357–362.
50. Vergarajauregui S, Connelly PS, Daniels MP, Puertollano R. Autophagic dysfunction in mucolipidosis type IV patients. *Hum Mol Genet* 2008;**17**:2723–2737.
51. Lam AP, Gottardi CJ. Beta-catenin signaling: a novel mediator of fibrosis and potential therapeutic target. *Curr Opin Rheumatol* 2011;**23**:562–567.
52. Trajkovic K, Dhaunchak AS, Goncalves JT, Wenzel D, Schneider A, Bunt G *et al*. Neuron to glia signaling triggers myelin membrane exocytosis from endosomal storage sites. *J Cell Biol* 2006;**172**:937–948.